



# A systematic analysis of hexavalent chromium adsorption and elimination from aqueous environment using brown marine algae (*Turbinaria ornata*)

K. Kumaraguru<sup>1</sup> · P. Saravanan<sup>1</sup> · R. Rajesh kannan<sup>2</sup> · V. Saravanan<sup>2</sup>

Received: 22 April 2021 / Revised: 12 July 2021 / Accepted: 19 July 2021 / Published online: 6 August 2021  
© The Author(s), under exclusive licence to Springer-Verlag GmbH Germany, part of Springer Nature 2021

## Abstract

In this study, chromium (VI) adsorption was explored using *Turbinaria ornata* as sorbent and the effects of parameters like temperature, sorbent size, contact time, sorbent dose, and agitation speed were improved using the response surface method. The optimal condition for maximum adsorption of Cr (VI) was found as solution temperature (33.6 °C), sorbent size (0.786 mm), contact time (215 min), agitation speed (117 rpm), and adsorbent dose (2.7 g/l). The maximum removal percentage was found to be 95.25%. The investigational data was also studied using various adsorption models. From the Langmuir model, it was observed that a maximum Cr (VI) uptake of 44.95 mg/g was achieved. Thermodynamic constraints such as  $\Delta G^\circ$ ,  $\Delta H^\circ$ , and  $\Delta S^\circ$  have been assessed and it has been originating that the sorption procedure was impulsive and heat releasing in nature. A high  $R^2$  value, low root mean square error (RMSE), and mean absolute percentage error (MAPE) suggest that the Cr (VI) adsorption follows the pseudo-first-order model. The characterization of adsorbent was studied by FTIR and SEM. The FTIR exposed the connection of some functional groups such as carboxylic acid, hydroxyl, and amino in the adsorption of Cr ions. From all of our data, we conclude that the *Turbinaria ornata* explored in this work displayed good potential for chromium elimination from synthetic solutions.

**Keywords** *Turbinaria ornata* · Chromium · Biosorption · Response surface methodology · Optimization

## 1 Introduction

The major worldwide ecological problem is due to the presence of heavy metal ions as contaminate in the water. Due to the increase in industrialization throughout the world, especially over a past few decades, production of more than ten thousand of new chemicals results annually. These new chemicals are utilized by chemical process industries and then discharged into the effluent stream. Also, increased consumption of various pesticides, salinity of road, lethal substances from mining locations, used motor oil, and chemical fertilizers in agriculture contributes towards the

contamination of groundwater. The rate of increase in the world population demands pressure on the limited water resources. Most importantly, it would be impossible to summarize the prime causes responsible for water pollution and other types of environmental degradation in any community [1]. The main aim of wastewater handling is to reject or decrease toxins to levels that do not cause any adverse effects on the aquatic environment. Due to the increase in the alertness health of human and environmental hazards allied with ecological impurities, stricter guidelines are essential to attain the demand for novel treatment knowledge to eliminate contaminants from wastewater [2].

The big issue for humans and aquatic lives is the release of heavy metals into the channel of water over industrial activities. The most harmful and lethal impurities are cadmium, chromium, copper, lead, and mercury. Among the top 16 toxic metals, chromium is one of them which cause health effects to human [3]. Cr (VI) is highly lethal compared with Cr (III) [4]. By reacting to the DNA structure block and few protein molecules, it defectively influences the human being. Cr (VI) toxicity has undesirable effects like irritation of the

✉ K. Kumaraguru  
kumaragurautt@gmail.com

<sup>1</sup> Department of Petrochemical Technology, University College of Engineering, BIT Campus, Anna University, Tamil Nadu, Tiruchirappalli, India

<sup>2</sup> Department of Chemical Engineering, Annamalai University, Annamalai Nagar, Tamil Nadu, India

skin, ulceration, asthma, and severe diarrhea. It damages the tissues of the kidney, the cardiovascular issues, the liver, and the nerve. Expose of high chromium in the digestive zone and lungs causes cancer [5–8]. Consequently, extensive discharges of chromium into water sources of drinking water are to be controlled by the use of permissible standards and a strict mechanism for ecological control [9]. The maximum admissible limit of Cr (VI) in drinking water is  $0.05 \text{ mg l}^{-1}$  (EPA). It is likely to eliminate lethal metals from the marine medium by various methods, such as electro dialysis, electrochemical precipitation, ultrafiltration, reverse osmosis, emulsion liquid membrane, and exchange of ions [10–15]. Compared to traditional techniques, biosorption has some major advantages. It has comparatively low costs, it is also effective in diluting solutions, it reduces the development of chemical and/or biological sludges, it does not need any addition of nutrients, the biosorbent may be regenerated, and it allows metals to be recovered [16–21].

Recently, several investigators have attained adequate removal of chromium (VI) by employing cheap, naturally and widely available biomass as sorbents like rice straw [22], *Sterculia guttata* shell [23], Gulmohar fruit shell [24], fish scales and eggshells [25], *Leucaena leucocephala*-activated carbon [26], mangrove leaf powder [27], garlic stem and horse chestnut shell [28], avocado kernel seeds, *Juniperus procera* sawdust, *Mangifera indica* bark and papaya peel [29], longan seed [30], and algae [31–34]. These adsorbents are more economic than the resins or activated carbon. Furthermore, most of these biomasses are composed of major components of functional groups joint with polysaccharides, proteins, hemicellulose, lignin, and cellulose [35].

The functional groups present in algae play a vital role in the selective surface attachment of the solute. Brown algae are well known for their superior ability, when compared to other types of algae, in the adsorptive removal of pollutants due to the presence of functional groups such as amine, carboxylic acid, hydroxyl, imidazole, phosphate, and phenolic, in their cell wall. This leads to increased affinity with the metal ions in the aqueous medium [36]. The algae are also available in plenty. The presence of functional groups and less cost makes algae a better choice for the adsorption process [36, 37]. So far, the brown alga, *Turbinaria ornata*, is not utilized for chromium (VI) sorption. Hence, the novelty of the present work is the use of these brown algae for the removal of chromium (VI) ions. The applications for batch adsorption were implemented under various criteria such as adsorbent quantity, time of influence, temperature, sorbent dosage, agitation speed, and pH. Additionally, this research completed kinetic models, adsorption equilibrium isotherms, SEM, FTIR, and thermodynamics study.

## 2 Materials and methods

### 2.1 Preparation of biosorbents

*Turbinaria ornata* was obtained from the CSMCRI (Central Salt and Marine Chemical Research Institute) research station of marine algae (Mandapam, Tamil Nadu, India). The collected algae were washed with water to remove contaminations. The cleaned *Turbinaria ornata* was sun-dried for 10 days. Then, the sun-dried algae were further dried at  $105 \text{ }^\circ\text{C}$ . Finally, the *Turbinaria ornata* was then chopped into small bits and a household mixer was employed to pulverize them. In this work, *Turbinaria ornata* in the range of 0.176 to 1.503 mm particle size (using 80 mesh and 10 mesh) was used without any chemical pretreatment for sorption experimentations.

### 2.2 Synthetic Cr (VI) solution

The synthetic Cr (VI) solution was prepared by dissolving the required quantity of  $\text{K}_2\text{Cr}_2\text{O}_7$  in double-distilled water. This solution was utilized for the preparation of other concentrations of Cr (VI) by dilution. The spectrophotometer was used to measure the metal concentration in the test solution at the wavelength of 540 nm [38]. All chemicals were obtained from MERCK (Delhi) including analysis grade  $\text{K}_2\text{Cr}_2\text{O}_7$ .

### 2.3 Response surface methodology (RSM)

In RSM, the central composite design was utilized to evaluate the effects of sorbent size, sorbent dose, temperature, contact time, and agitation speed concurrently covering the spectrum of variables for chromium removal. The ranges of these factors were evaluated by Eq. (1) [39]:

$$x_i = \frac{X_i - X_0}{\Delta X} \quad (1)$$

where  $x_i$  is the coded value of the  $i^{\text{th}}$  variable and  $X_i$  and  $X_0$  are uncoded values of the  $i^{\text{th}}$  variable and  $i^{\text{th}}$  variable at the center point respectively.

The range and levels of individual variables were given in Table 1.

A quadratic polynomial Eq. (2) was formed by applying the RSM to forecast the efficiency as a function of variables.

$$y = \beta_0 + \sum_{i=1}^K \beta_i X_i + \sum_{i=1}^K \beta_{ii} X_i^2 + \sum_{i=1}^{K-1} \sum_{j=2}^K \beta_{ij} X_i X_j \quad (2)$$

**Table 1** Range of factors for Cr (VI) sorption

Independent variable		Levels and range				
		−2.38	−1	0	+1	+2.38
Sorbent dosage (g/100 ml)	$X_1$	0.1	0.2	0.3	0.4	0.5
Average sorbent size (mm)	$X_2$	1.503	1.057	0.564	0.389	0.176
Agitation speed (rpm)	$X_3$	50	100	150	200	250
Temperature (°C)	$X_4$	25	30	35	40	45
Contact time (h)	$X_5$	2	4	6	8	10

where  $Y$  is the predicted Cr (VI) removal efficiency and  $\beta_i$ ,  $\beta_j$ , and  $\beta_{ij}$  are coefficients which denote the linear, quadratic, and cross products of  $x_1$ ,  $x_2$ , and  $x_3$  on response.

The response model coefficient was assessed using a multiple regression analysis system that was comprised in the RSM. The fit quality of the models was assessed from their correlation and determination coefficients.

Different statistical analytical methods were used to find the investigational error, model fitness, and statistical implication of the terms in the model when fitting the model. The model was confirmed through the statistical tests called variance analysis (ANOVA). The importance of any term in the equation is to assess in each case the morality of fit. Response surfaces have been drawn to estimate the individual and interactive effects of factors on chromium removal efficiency.

## 2.4 Batch experimentation

Trials were conducted as per the software of design experts (Stat Ease, 8.0.5 USA). A desired amount of marine algae (0.1–0.5 g), as per the design given in Table 2, was added into each 250-ml conical flasks containing 100 ml of 100 ppm Cr (VI) solution. A water bath shaker was employed for agitation and maintaining the temperature of the solution as per the design. The speed was varied between 50 and 250 rpm. The substances in the flask were centrifuged at 4000 rpm for 3 min after biosorption and the solution was separated from biomass and analyzed.

The separated solution was examined at 540 nm for Cr (VI) concentration using a UV–Vis spectrophotometer (SHIMADZU UV -2450). The absorbance value for initial and final Cr (VI) concentration was found. The triplicate mean value of the experiments was reported.

The Cr (VI) removal was estimated by Eq. (3):

$$Y(\%) = \frac{C_0 - C_i}{C_0} \times 100 \quad (3)$$

The uptake,  $q_e$  (mg/g), was estimated by Eq. (4):

$$q_e = \frac{V(C_0 - C_e)}{M} \quad (4)$$

where  $C_0$  (mg/l) is the initial Cr (VI) concentration and  $C_e$  (mg/l) is the equilibrium Cr (VI) concentration.  $Y$  is the removal efficiency in percentage,  $V$  (L) is the solution volume, and  $M$  (g) is the biomass weight.

## 2.5 Point of zero charge (pH<sub>ZPC</sub>) and pH effect

The point of zero charge of sorbent (pH<sub>ZPC</sub>) was found at different pH ranging from (2 to 12) using the procedure given by Sarojini and coworkers [40]. The pH effect was studied at the optimized conditions of other parameters. The influence of solution pH was analyzed at optimum conditions for a pH range (2 to 7). The pH was attuned by adjusting essential amounts of acid or base.

## 2.6 Biosorbent characterization

### 2.6.1 Scanning electron microscope

SEM for new and algae loaded with Cr (VI) was taken. Dehydrated biosorbent samples were tested using a SEM (JEOL JSM 6360 Japan) by standard procedure.

### 2.6.2 Study by Fourier transform infrared spectroscopy

The FTIR spectrometer (Perkin-Elmer Spectrum One FT-IR 4200) was engaged to investigate the category of functional groups responsible for adsorption in biomass. The investigation was made between 4000 and 400  $\text{cm}^{-1}$ .

## 2.7 Thermodynamics of Cr (VI) sorption

At optimum conditions, the temperature has been varied from 293 to 313 K in order to study the thermodynamic aspects of the sorption process.

$$\Delta G^\circ = -RT \ln K_C \quad (5)$$

where  $\Delta G^\circ$  is the standard Gibbs free energy (kJ/mol),  $\Delta H^\circ$  is the enthalpy changes (kJ/mol), and  $\Delta S^\circ$  is the entropy (kJ/mol K). The following equations (Eqs. (6) and (7)) were employed to find the properties [41]:

**Table 2** CCD for sorption of Cr (VI)

Obs	$X_1$	$X_2$	$X_3$	$X_4$	$X_5$	Cr (VI) removal, %	
						Experimental	Theoretical
1	0.00	0.00	0.00	0.00	0.00	95.25	94.85
2	1.00	1.00	-1.00	-1.00	1.00	62.55	73.97
3	1.00	-1.00	-1.00	1.00	1.00	59.26	58.39
4	-1.00	-1.00	1.00	-1.00	-1.00	98.55	82.48
5	1.00	1.00	1.00	-1.00	1.00	69.33	69.2
6	-1.00	-1.00	-1.00	-1.00	1.00	63.33	66.3
7	-1.00	-1.00	1.00	-1.00	1.00	69.33	77.38
8	0.00	0.00	0.00	0.00	0.00	95.25	94.85
9	0.00	0.00	0.00	0.00	0.00	95.25	94.85
10	-1.00	1.00	1.00	-1.00	-1.00	67.65	71.51
11	-1.00	1.00	-1.00	-1.00	1.00	67.49	63.84
12	1.00	-1.00	1.00	1.00	1.00	50.55	56.1
13	1.00	-1.00	1.00	1.00	-1.00	49.56	56.31
14	0.00	0.00	0.00	0.00	2.38	59.38	56.89
15	-1.00	-1.00	-1.00	-1.00	-1.00	69.46	76.41
16	-1.00	1.00	1.00	-1.00	1.00	62.25	72.01
17	0.00	0.00	0.00	0.00	0.00	95.25	94.85
18	1.00	-1.00	-1.00	-1.00	-1.00	59.89	69.038
19	0.00	0.00	0.00	0.00	0.00	95.25	94.85
20	-2.38	0.00	0.00	0.00	0.00	58.89	56.37
25	1.00	-1.00	1.00	-1.00	1.00	68.22	68.44
26	-1.00	-1.00	1.00	1.00	1.00	62.36	63.77
27	-1.00	-1.00	-1.00	1.00	-1.00	69.55	69.69
28	1.00	1.00	-1.00	1.00	-1.00	59.88	65.25
29	0.00	0.00	0.00	0.00	-2.38	65.99	62.43
30	1.00	1.00	-1.00	-1.00	-1.00	68.55	67.18
31	1.00	-1.00	-1.00	1.00	-1.00	62.63	63.57
32	-1.00	1.00	-1.00	1.00	-1.00	63.88	65.21
33	1.00	1.00	1.00	-1.00	-1.00	48.77	57.5
34	-1.00	1.00	1.00	1.00	1.00	62.55	61.99
35	-1.00	-1.00	1.00	1.00	-1.00	65.69	75.19
36	2.38	0.00	0.00	0.00	0.00	49.23	45.75
37	0.00	0.00	0.00	0.00	0.00	95.25	94.85
38	-1.00	1.00	-1.00	1.00	1.00	48.88	54.42
39	1.00	1.00	1.00	1.00	1.00	58.44	60.45
40	0.00	2.38	0.00	0.00	0.00	98.55	95.67
41	0.00	0.00	-2.38	0.00	0.00	70.56	73.97
42	0.00	0.00	2.38	0.00	0.00	68.23	64.07
43	1.00	-1.00	-1.00	-1.00	1.00	69.23	70.24
44	0.00	0.00	0.00	-2.38	0.00	65.58	61.55
45	0.00	0.00	0.00	2.38	0.00	51.16	43.49
46	-1.00	1.00	-1.00	-1.00	-1.00	59.23	68.33
47	0.00	0.00	0.00	0.00	0.00	95.25	94.85
48	1.00	1.00	1.00	1.00	-1.00	55.13	54.98
49	1.00	1.00	-1.00	1.00	1.00	59.14	65.72
50	-1.00	-1.00	-1.00	1.00	1.00	52.25	53.29
51	0.00	0.00	0.00	0.00	0.00	95.25	94.85
52	1.00	-1.00	1.00	-1.00	-1.00	58.56	62.24

**Table 3** Analysis of variance (ANOVA) for response surface quadratic model

Source	Sum of squares	Df	Mean square	F value	p-value Prob > F
Model	10,566.56	20	528.33	71.45	< 0.0001
A	215.33	1	215.33	29.12	< 0.0001
B	35.7	1	35.7	4.83	0.0356
C	1.69	1	1.69	0.23	0.6356
D	655.12	1	655.12	88.59	< 0.0001
E	57.63	1	57.63	7.79	0.0089
AB	77.31	1	77.31	10.46	0.0029
AC	330.76	1	330.76	44.73	< 0.0001
AD	2.82	1	2.82	0.38	0.5414
AE	254.7	1	254.7	34.44	< 0.0001
BC	16.73	1	16.73	2.26	0.1426
BD	25.92	1	25.92	3.51	0.0706
BE	62.55	1	62.55	8.46	0.0067
CD	0.69	1	0.69	0.093	0.762
CE	49.8	1	49.8	6.73	0.0143
DE	79.82	1	79.82	10.79	0.0025
A <sup>2</sup>	3505.61	1	3505.61	474.08	< 0.0001
B <sup>2</sup>	234.48	1	234.48	31.71	< 0.0001
C <sup>2</sup>	1789.32	1	1789.32	241.98	< 0.0001
D <sup>2</sup>	3311.45	1	3311.45	447.82	< 0.0001
E <sup>2</sup>	2260.67	1	2260.67	305.72	< 0.0001
Residual	229.23	31	7.39		
Lack of fit	229.23	22	10.42		
Pure error	0	9	0		
Cor total	10,795.79	51			

$$K = q_e / C_e \tag{6}$$

$$\ln K = \frac{\Delta S^\circ}{R} - \frac{\Delta H^\circ}{RT} \tag{7}$$

### 2.8 Regeneration

The reusability of the biosorbent was studied using HCl in the concentration range of 0.1 to 0.5 M. The experimental cycle of sorption–desorption was repeated till five cycles and the quantity of desorbed metal was estimated. The desorption efficiency was found using Eq. (8) [42, 43].

$$\text{Desorption efficiency} = \frac{\text{Quantity of Cr (VI) desorbed}}{\text{Quantity of Cr (VI) adsorbed}} \times 100 \tag{8}$$

### 2.9 Equilibrium isotherm study

Langmuir, Freundlich, Dubinin-Radushkevich (DR), and Temkin isotherms were used to find the lined isotherms specifically, to regulate the Cr (VI) sorption mechanism on to marine algae.

#### 2.9.1 Langmuir isotherm

Langmuir [44] planned a philosophy to define the sorption on metal surfaces of the vapor molecules. The isotherm Langmuir adsorption has successfully been used in many other real monolayer adsorption sorption processes. Langmuir’s adsorption model is assumed that inter-molecular forces decrease quickly with distance, thus predicting that the adsorbed monolayer covers exist on the outside surface of the adsorbent. Sorbent has a finite *c* in theory. Equation (9) defines the Langmuir isotherm.

$$q_e = \frac{q_{\max} K_a C_e}{1 + K_a C_e} \tag{9}$$

where *C<sub>e</sub>* (g/l) is the equilibrium concentration of Cr (VI), *q<sub>e</sub>* (g/g) is the equilibrium metal uptake quantity, *q<sub>max</sub>* (mg/g), and *K<sub>a</sub>* (L/mg) are Langmuir constants, respectively, connected to sorption volume and sorption energy. The equilibrium (*q<sub>e</sub>*) is estimated using Langmuir isotherm from the experimental data.

#### 2.9.2 Freundlich isotherm

Freundlich [45] reported the empirical calculation used to define non-homogenous systems.

$$q_e = K_F C_e^{1/n} \tag{10}$$

where *K* (mg/g) is the capacity of biosorption and 1/*n* (mg/g) is a measure of the intensity of sorption. Favorable adsorption means the value of *n* should be between 1 and 10.

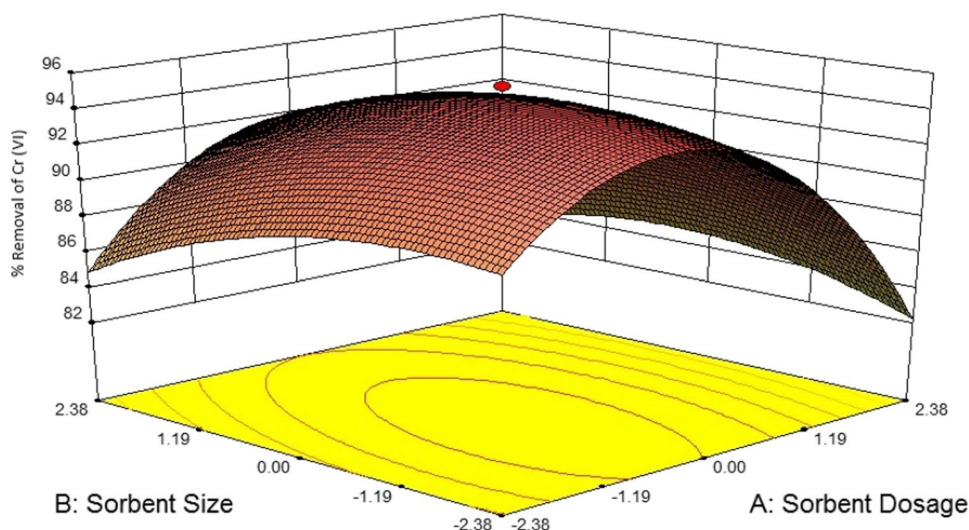
#### 2.9.3 D-R isotherm

The isotherm *D-R* [46] is given by,

$$\begin{aligned} q_e &= q_m \exp(-D\varepsilon^2) \\ \varepsilon &= RT \ln(1 + 1/C_e) \end{aligned} \tag{11}$$

where *D* is the isotherm constant Dubinin-Radushkevich (gmmol/J) and *q<sub>m</sub>* is the maximum sorption capacity (mg/g).

**Fig. 1** Effect of sorbent dosage and sorbent size on Cr (VI) removal



The constant  $D$  gives the mean free adsorption energy per adsorbate molecule.

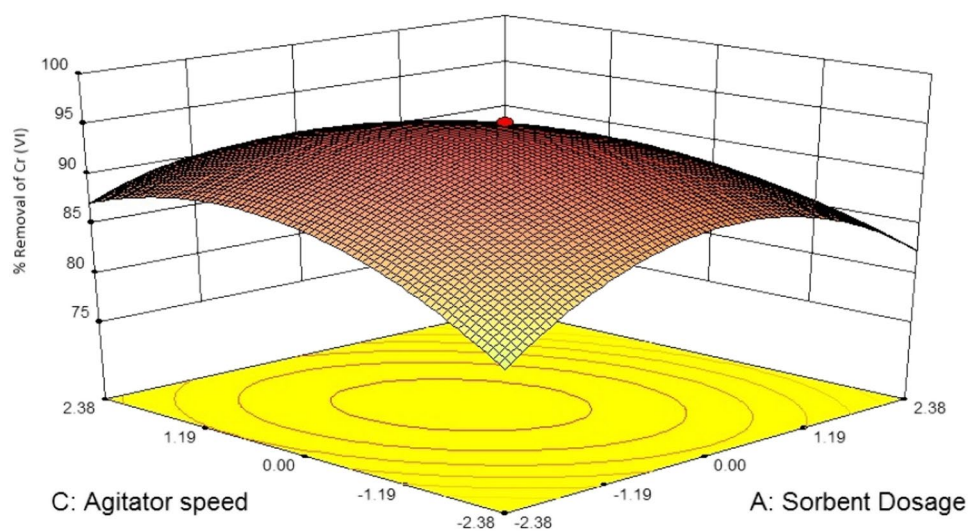
#### 2.9.4 Temkin isotherm

The Temkin isotherm [47] is

$$q_e = \frac{RT}{\Delta Q} \ln(K_T C_e) \quad (12)$$

where  $K_T$  is the Temkin model constant (L/mg),  $Q$  is the adsorption heat (J),  $q_e$  is the equilibrium adsorbent amount (mg/g),  $R$  is the universal gas constant (J/gmmole-K), and  $T$  is the temperature (K).

**Fig. 2** Effect of sorbent dosage and agitation speed on Cr (VI) removal



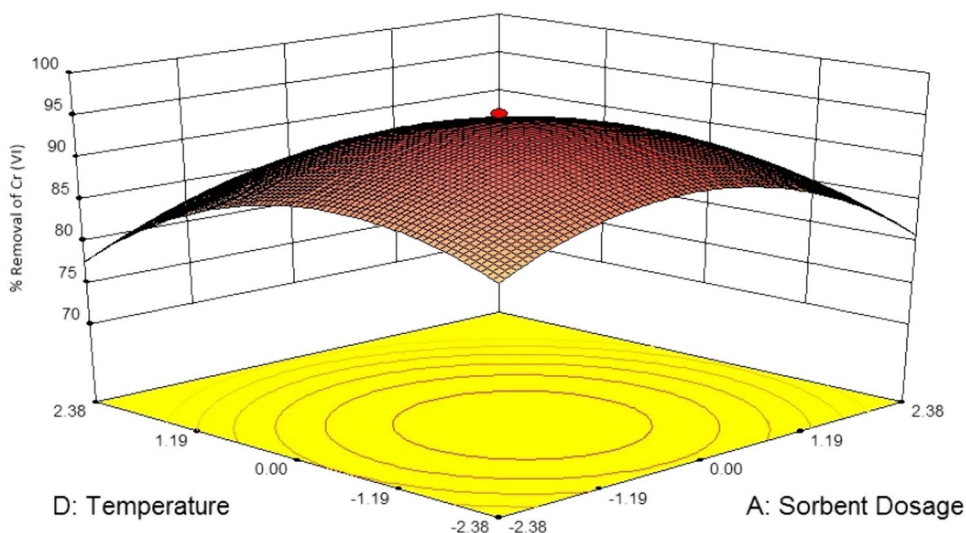
### 3 Results and discussion

#### 3.1 Statistical analysis for Cr (VI) sorption onto *Turbinaria ornata*

CCD has been used to study the effects of factors considered in this study, on Cr (VI) sorption. In Table 1, a summary of the independent parameters and their range and level was presented. The five parameters remained identified as potential parameters for Cr (VI) sorption from the results of previous literature [48].

Table 2 shows the experimental result obtained from each trial and Cr (VI) removal predicted by the II-order polynomial equation which relates the response with the five different independent process variables. Equation (13) gives the

**Fig. 3** Effect of sorbent dosage and temperature on Cr (VI) removal



mathematical model associated with the percentage removal of Cr (VI) ions.

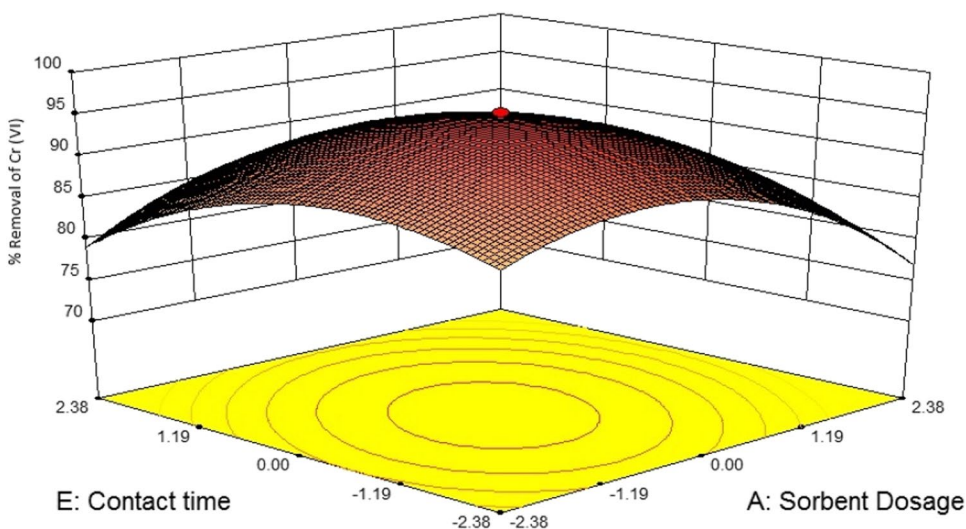
The regression equation for the determination of output response for Cr (VI) was found as follows.

$$\begin{aligned}
 \text{Cr (VI) removal efficiency, \%} = & 94.85 - 2.23 * A - 0.91 * B \\
 & + 0.20 * C - 3.89 * D - 1.15 * E \\
 & + 1.55 * A * B - 3.22 * A * C \\
 & + 0.30 * A * D + 2.82 * A * E \\
 & - 0.72 * B * C + 0.90 * B * D \\
 & + 1.40 * B * E - 0.15 * C * D \\
 & + 1.25 * C * E - 1.58 * D * E \\
 & - 7.73 * A^2 - 2.00 * B^2 - 5.52 * C^2 \\
 & - 7.51 * D^2 - 6.21 * E^2
 \end{aligned}
 \tag{13}$$

### 3.2 Analysis of variance (ANOVA)

From Table 3, the importance of the model was suggested by the model *F*-value of 71.45. Standards of “Prob > *F*” less than 0.05 specify model terms are important. The significant terms were identified based on the *F* value, whose value less than 0.05 shows the importance of the term for the sorption process. The linear effect of sorbent dose, sorbent size, temperature and contact time, the square effect of all the terms, and interactive effect of AB, AC, AE, BE, CE, and DE are found to be important for the Cr (VI) sorption process using *Turbinaria ornata*. The predicted *R*<sup>2</sup> value of 0.9127 is in line with the adjusted *R*<sup>2</sup> value of 0.9651.

**Fig. 4** Effect of sorbent dosage and contact time on Cr (VI) removal



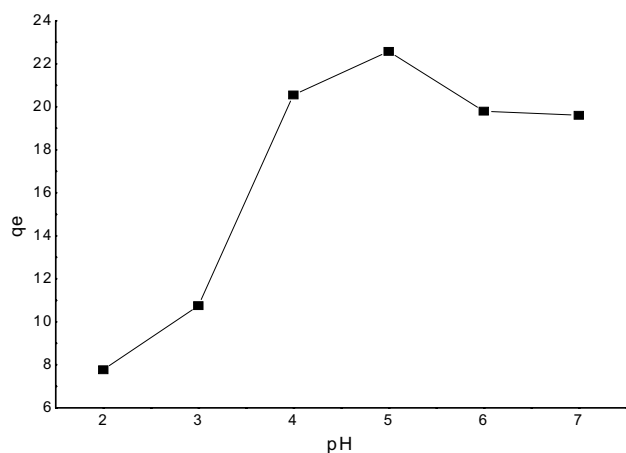


**Fig. 5** Effect of pH on the sorption capacity of *Turbinaria ornata*

### 3.3 Optimization of process variables for Cr (VI) removal using *Turbinaria ornata*

Brown marine algae, *Turbinaria ornata*, biosorption capacity was investigated by means of various factors like sorbent dosage, average sorbent size, agitation speed, temperature and contact time using surface plots (Figs. 1, 2, 3, and 4). The plots of the surface response were signified as a function of two features at a time, keeping other features at fixed levels. The surface response curve nature dictates the interaction between the factors [31]. The oval shape is well interactive and the circular curve does not interact with the two variables. It has been observed from plots that the elliptical contour shows the mutual interaction of all the parameters. There was a virtual important interaction between each of the two parameters, and the maximum projected to yield as specified in the contour diagrams by the surface confined in the smallest ellipse [31].

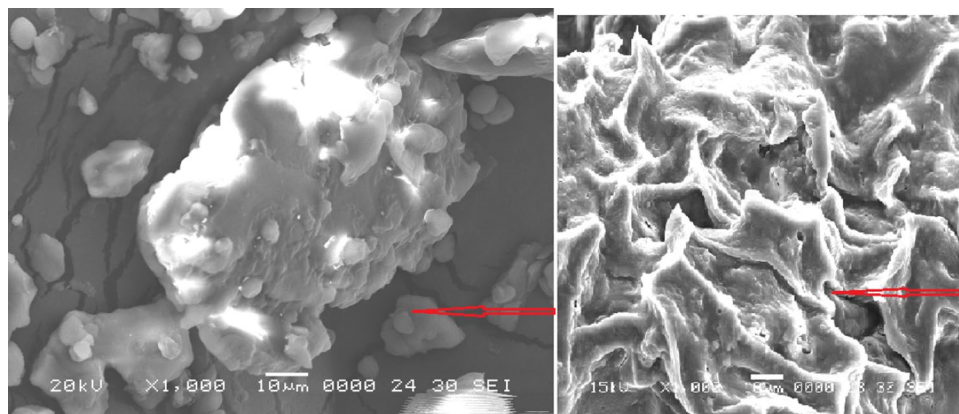
The degree of coefficients in Eq. (13) shows the positive and negative contributions of factors. All the variables' quadratic terms have a negative influence on chromium removal. In addition, the interactions' outcome of "sorbent dosage–agitation speed" and "sorbent dosage–contact time" has a positive influence. The interactions of "sorbent dosage–agitation speed," "sorbent size–temperature," "sorbent size–contact time," "agitation speed–contact time," "sorbent dose–temperature," "agitation speed–temperature," "sorbent size–agitation speed," "sorbent size–contact time," "sorbent dose–temperature," "agitation speed–contact time," "sorbent size–agitation speed," "agitation speed–temperature," and "temperature–contact time" have a negative influence on chromium elimination.

Figure 1 depicts the interactive effect of sorbent dose and size on Cr (VI) elimination. The outcomes indicate that Cr (VI) removal varies from 84 to 93% for the sorbent dosage 0.1 to 0.2 g/100 ml. Hence, the optimum sorbent dose is 2.7 g/l. Addition of seaweed above this quantity decreases the sorption of *Turbinaria ornata*. This may be due to the splitting effect of the concentration gradient between sorbate and sorbent with increasing seaweed concentration causing a decrease in the amount of chromium adsorbed onto the unit weight of *H. valentiae* [31]. This indicates that the sorbent dose had a vital effect on the uptake capacity of metal in adsorption [36].

The impact of agitation speed was investigated in the rpm range of 50 to 250. From Fig. 2, it was inferred that the maximum Cr (VI) elimination happens at 117 rpm. At very low agitation, the biomass accumulates at the bottom and decreases the Cr (VI) removal. But at higher agitation, the Cr (VI) elimination increases due to homogeneous suspension of sorbent in the solution. This is well supported by Jayakumar and groups [49].

From Fig. 3, it was clear that Cr (VI) elimination improved from 75 to 92% with an escalation in temperature

**Fig. 6** SEM picture of *Turbinaria ornata*. **A** Before adsorption. **B** After adsorption

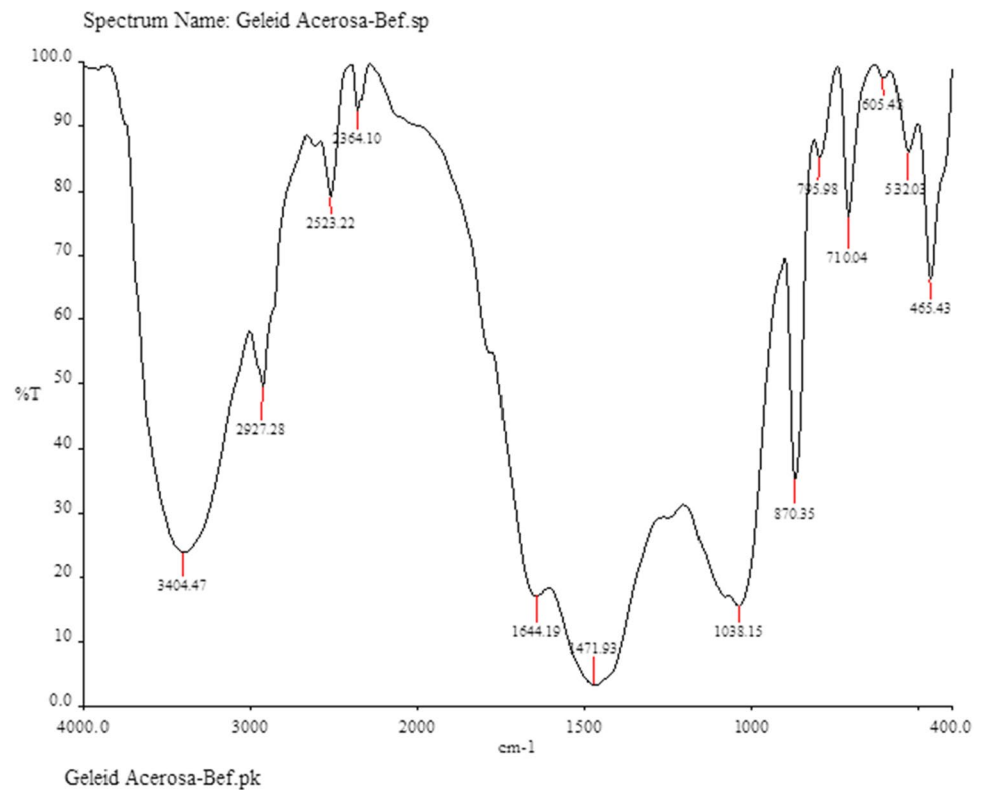


**A)** Before adsorption

**B)** After adsorption



**Fig. 7** FTIR picture of virgin *Turbinaria ornata*

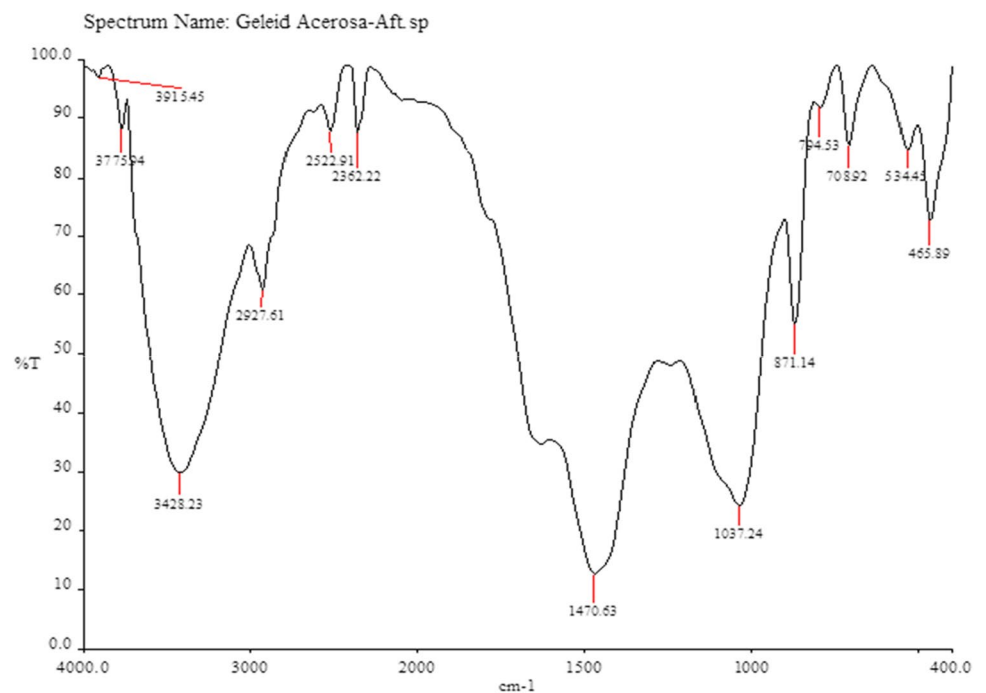


from 25 to 33.6 °C. A maximum elimination of 93% Cr (VI) is found at 33.6 °C. It shows that sorption may be a combination of both chemical and physical adsorption. At higher temperature, the pores in the *Turbinaria ornata* enlarge

lead to an increase in surface area that in turn enhances the uptake of Cr (VI) ions [50].

In Fig. 4, it has been inferred that the elimination of Cr (VI) increased with an increment in contact time of up to 215 min. Furthermore, there is no appreciable change in the

**Fig. 8** FTIR picture of Cr (VI)-loaded *Turbinaria ornata*



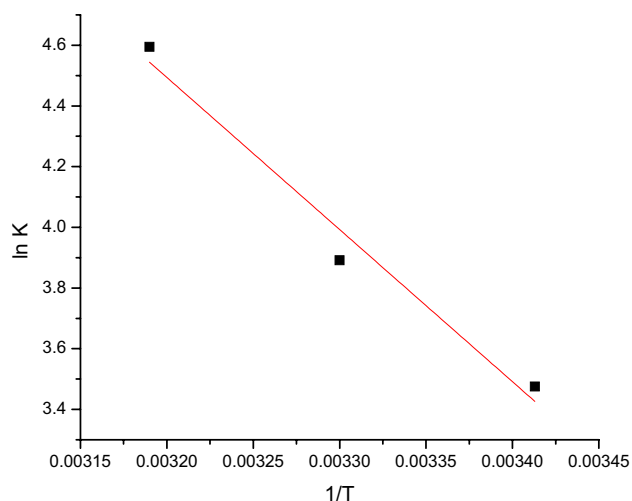


**Fig. 9** Thermodynamics investigation on the sorption of Cr (VI) by *Turbinaria ornata*

elimination of Cr (VI). Hence, a contact time of 215 min was found to be optimum. The plots (Figs. 1, 2, 3 and 4) also reveal that the optimum condition lies within the region mentioned in Table 1.

The Bhatti group [51] reported the mass transfer resistance among the aqueous and solid phases overwhelms owing to the initial metal concentration at high in solution performances as a driving force to transfer ions from the bulk solution to the sorbent surface. Similar results were achieved for the adsorption of Cr in Pakade and coworkers [52].

Using RSM, optimum conditions were obtained for the elimination of Cr (VI) using *Turbinaria ornata*. The best values found by replacing the particular coded parameter values are sorbent size at 0.7860 mm, sorbent dosage at 0.27 g/l, temperature at 33.6 °C, contact time at 215 min, and agitation speed at 117 rpm. The higher percentage deletion of chromium was obtained at this condition. It was found that the optimum values predicted from MATLAB are within the proposal area.

### 3.3.1 Effect of pH on biosorption

At isoelectric point (IEP), zeta potential is equal to zero. Zeta potential was evaluated at various pH from 2 to 12

**Table 4** Thermodynamic properties of Cr (VI) sorption by *Turbinaria ornata*

T, K	$\Delta G$ (kJ/mol)	$\Delta H$ (kJ/mol)	$\Delta S$ (kJ/mol K)
293	-8.4675	41.675	0.1707
303	-9.804		
313	-11.958		

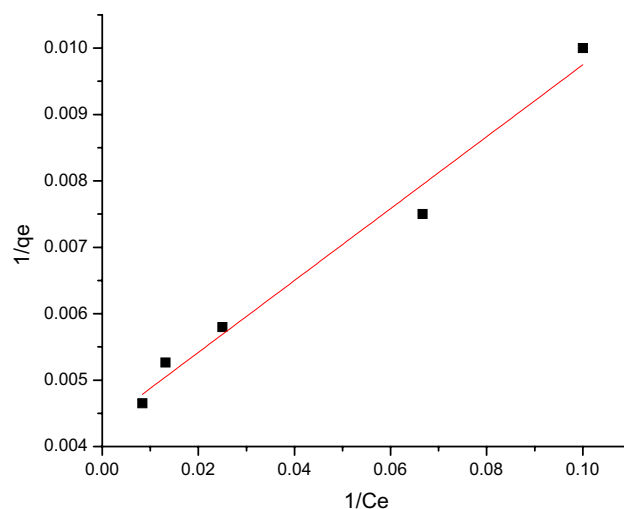


**Fig. 10** Langmuir plot for biosorption of Cr (VI) on *Turbinaria ornata*

and the  $\text{pH}_{\text{zpc}}$  of the sorbent was found to be 4.7. This is well supported by [53]. Above this zero-point charge, the surface of algae is negatively charged, and at lower pH, the surface charge is positive.

The influence of pH was depicted in Fig. 5. In this study, the elimination of Cr (VI) metal ions using *Turbinaria ornata* was studied by changing the pH from 2 to 7.

**Table 5** Isotherm constant and their values at a temperature of 308.15 K

Isotherm model	Parameters	Values
Langmuir	$q_m$ (mg/g)	44.95
	$K_a$	0.0799
	$R^2$	0.97578
	RMSE	1.9418
	MAPE	3.2%
Freundlich	$K_f$	1.77033
	$1/n$	0.27677
	$R^2$	0.90148
	RMSE	6.523
	MAPE	16.32%
Dubinin-Radushkevich	$q_m$ (mg/g)	40.42
	$B$	-256.5
	$E$	0.044
	$R^2$	0.65061
	RMSE	14.235
	MAPE	34.22%
Temkin	$B$	43.4191
	$k_T$	1.1993
	$R^2$	0.97553
	RMSE	1.9522
	SSE	3.3%

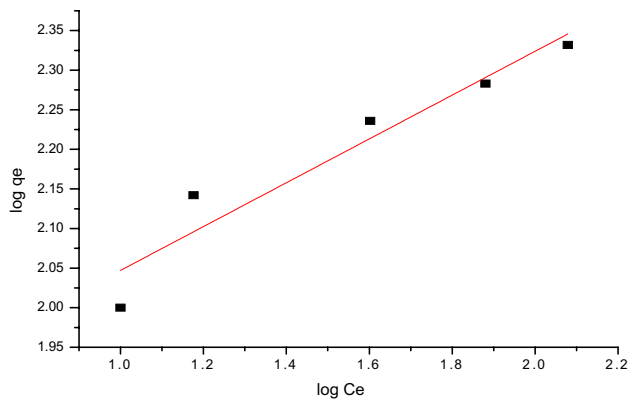


**Fig. 11** Freundlich plot for biosorption of Cr (VI) on *Turbinaria ornata*

The maximum biosorption capacity of *Turbinaria ornata* for Cr (VI) ions was 99% at pH 5. At lower and higher pH values, the sorption efficiency was significantly reduced. As the pH increases from 2, on *Turbinaria ornata*, the Cr ion biosorption rises and reaches the maximum at pH 5. The increased efficiency of biosorption at pH 5 may be due to more negative binding of more positively charged metal ions on the biomass surface. In the pH, 2.0–7.0, Cr (VI) primarily occurs in the form of  $\text{HCrO}_4^-$ ,  $\text{H}_2\text{CrO}_4^-$ , and  $\text{CrO}_2^-$ , but  $\text{HCrO}_4^-$  dominates. Therefore, the Cr (VI) adsorption is found to be maximum at acidic conditions. This is due to the electrostatic attraction between  $\text{HCrO}_4^-$  and positively charge adsorbent surface. The Cr (VI) ions biosorption onto *Turbinaria ornata* was decreased at pH values greater than 5. This is in accordance with Murphy et al. [54].

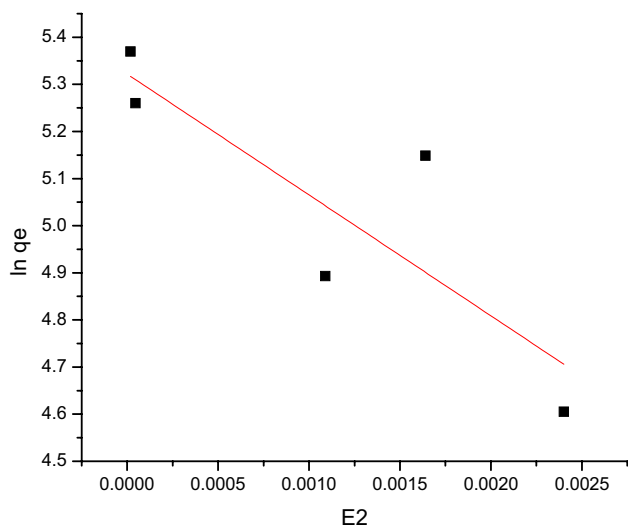


**Fig. 12** Dubinin-Radushkevich isotherms for biosorption of Cr (VI) on *Turbinaria ornata*

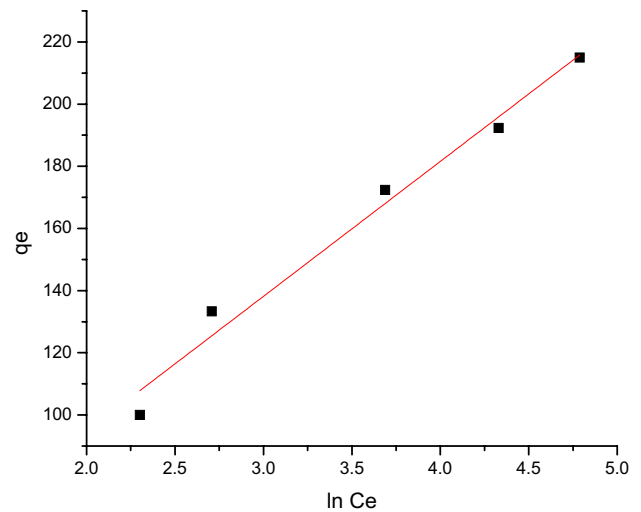


**Fig. 13** Temkin isotherm for biosorption of Cr (VI) on *Turbinaria ornata*

### 3.4 Characterization of the biosorbent and mechanism of biosorption

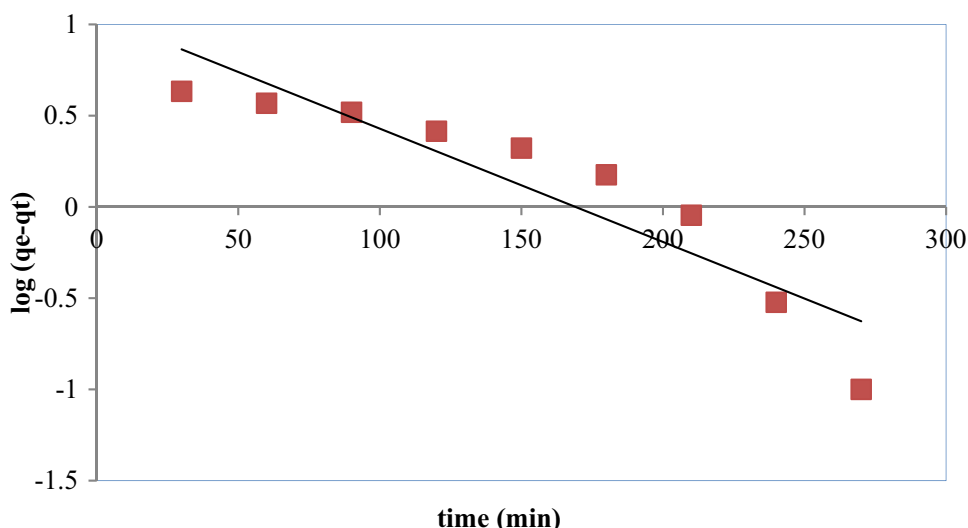
#### 3.4.1 SEM analysis

Figure 6 represents the SEM micrographs if before and after sorption experimentation. Before the adsorption of Cr (VI), the surface of algae is uneven and has a permeable surface. After sorption, the pores are occupied on the surface of *Turbinaria ornata*. It suggests that the sorption of Cr (VI) occurs on *Turbinaria ornata*. Moreover, the formation of a molecular cloud on the algae surface agrees on the binding

**Table 6** Comparison of Cr (VI) uptake by various biomass

Adsorbent	Adsorption capacities (mg/g)	Reference
Rosehip seed shell	15.17	[62]
Bentonite	48.83	[63]
Natural sepiolite	37	[64]
Eggshell	10.33	[65]
Papaya peels	7.160	[66]
Banana peel	10.42	[62]
Ground nutshell	3.792	[67]
Musa acuminate bract	36.84	[68]
<i>Irvingia gabonensis</i> stem bark	23.26–26.18	[69]
Sagwan sawdust biochar	9.62	[70]
Bacillus strain biosorbent	106.38	[71]
Pongamia pinnata shell	96.2	[72]
Amorphous silica nanoparticles	34	[73]
Rosehip seed shell	15.17	[62]
<i>Turbinaria ornata</i>	44.95	Present work

**Fig. 14** PFO model for Cr (VI) sorption onto *Turbinaria ornata*



of Cr (VI) ions to the functional groups existing in *Turbinaria ornata*. In the Murphy group, similar results for Cr-loaded seaweed have been obtained [55].

### 3.4.2 FTIR spectra analysis

The changes in the functional groups present in the adsorbent were determined by the FTIR spectra of *Turbinaria ornata*, before and after Cr (VI) sorption. The sorbent spectra were determined in the range of 400–4000  $\text{cm}^{-1}$ . All the spectra for the raw and Cr (VI) charged biomass were shown in Figs. 7 and 8. The FTIR spectra of *Turbinaria ornata* exhibited a number of absorption peaks, representing the adsorbent's complex nature. Figure 7 and 8 show the basic adsorbent peaks before and after *Turbinaria ornata*. The absorption peak around 3428.23 and 1470.63  $\text{cm}^{-1}$  was specified that being free and inter-molecular bonded hydroxyl groups played a vital role in the elimination of chromium (VI) [56].

### 3.5 Thermodynamic study for biosorption of Cr (VI) ions by *Turbinaria ornata*

Standard enthalpy ( $\Delta H^\circ$ ) and entropy ( $\Delta S^\circ$ ) were estimated from the intercept and slope of the plot,  $\ln K$  vs  $T^{-1}$ , as shown in Fig. 9 and presented in Table 4.

The values of  $\Delta G^\circ$  were obtained at 293, 303, and 413 K. The negative standard Gibbs free energy value shows the viability of the sorption and the impulsive nature of Cr (VI) sorption. The positive value of  $\Delta H^\circ$ , which represents the binding of Cr (VI) to algae, was endothermic. This is in accordance with the literature [57, 58]. The positive entropy shows the increase in randomness at the solid/liquid boundary during biosorption [58].

## 3.6 Biosorption isotherms

### 3.6.1 Langmuir isotherm

Figure 10 shows the Langmuir plot for different initial metal concentrations of Cr (VI) sorption using *Turbinaria ornata*. The constants  $q$  and  $b$  are tabulated in Table 5. The constant  $b$  has represented the affinity between sorbent and sorbate. In the present Cr (VI) sorption work, *Turbinaria ornata* has high uptake ( $q$ ) for Cr (VI). Also, the coefficient of determination ( $R^2$ ) is high for Langmuir isotherm.

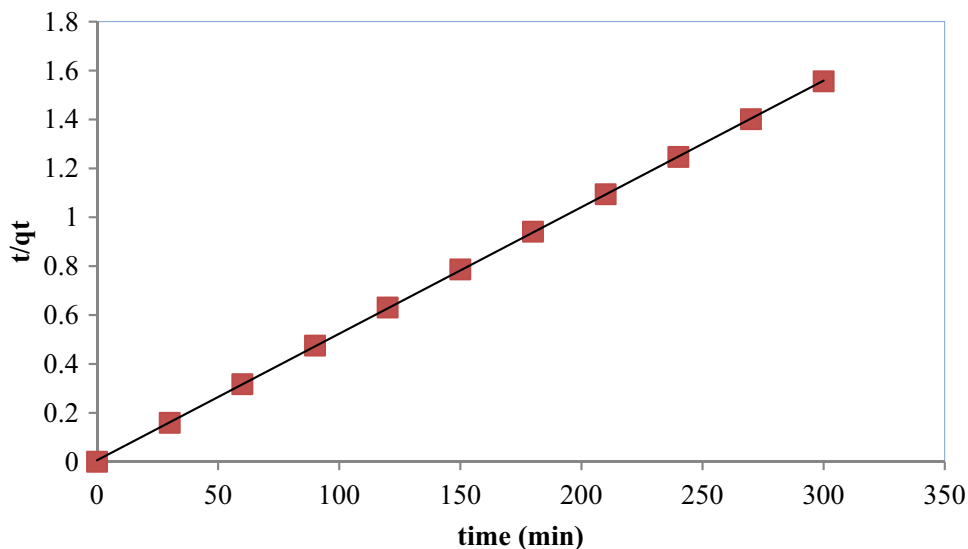
### 3.6.2 Freundlich isotherm

Figure 11 shows the Freundlich plot of Cr (VI) sorption isotherms for *Turbinaria ornata* and the values of constants  $K_f$  and  $1/n$  were provided in Table 5.  $K_f$  is a constant relating to the capacity of sorption and  $1/n$  is an empirical parameter

**Table 7** Kinetic parameters for Cr (VI) sorption on to *Turbinaria ornata*

Pseudo-first order	
$K_1$ ( $\text{min}^{-1}$ )	37.79
$R^2$	0.9862
RMSE	3.245
MAPE	5.65%
Pseudo-second order	
$k_2 \times 10^4$	1.52
$R^2$	0.9758
RMSE	5.645
MAPE	8.65%
IPD	
$k_d$ ( $\text{mg/g min}^{-0.5}$ )	1.726
$R^2$	0.9491
RMSE	13.245
MAPE	16.21%

**Fig. 15** Pseudo-II-order model for Cr (VI) sorption onto *Turbinaria ornata*



relating to the intensity of sorption which varies with the heterogeneity of the material. The value of  $K_f$  was found to be 1.77033 from the graphs and the value of  $1/n$  was found to be 0.27677. The  $1/n$  value between 0 and 1 usually indicates good sorption. In this work, a value of 0.27977 specifies that the sorption of Cr (VI) onto *Turbinaria ornata* was feasible [59].

### 3.6.3 Dubinin-Radushkevich isotherm

Figure 12 demonstrates the plot of  $\ln q_e$  versus  $E^2$ , from which the  $D-R$  constants,  $\beta$ , and  $q_m$  were estimated from the intercept and slope respectively and the values were given in Table 5. The energy value obtained in this work has  $E < 8$  kJ/mol, which indicates that Cr (VI) sorption was physical since an  $E > 8$  kJ/mol represents chemical adsorption [60, 61].

### 3.6.4 Temkin isotherm

Figure 13 shows the plot of  $q_e$  versus  $\ln C_e$ , and the constants were estimated and presented in Table 5. The Langmuir model

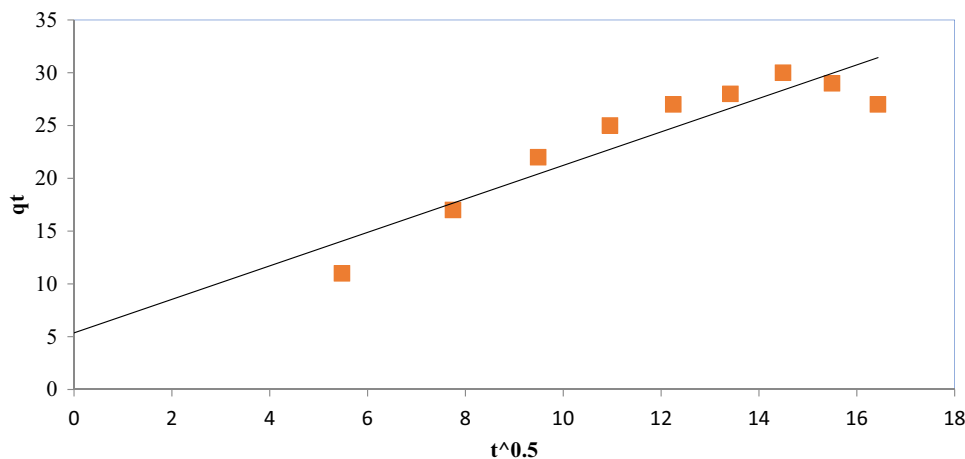
therefore provides the best correlation factors between the four isotherm models based on high  $R^2$  value and low RMSE and MAPE values.

A comparison has been made based on uptake of Cr (VI) with some other cheap biomass and they are given in Table 6. From the comparison, it has been observed that the brown algae *Turbinaria ornata* have better sorption capacity than most of the cheap biomass utilized for Cr (VI) adsorption.

## 4 Sorption kinetics

The optimal time (balance) helps to determine the binding process rate. To establish the mechanism for the sorption process, several kinetic models are required. Three kinetic models were employed to investigate Cr (VI) sorption kinetics in *Turbinaria ornata*: pseudo-first, pseudo-second, intra-particle diffusion (IPD).

**Fig. 16** IPD model for the sorption of Cr (VI) on *Turbinaria ornata*



#### 4.1 Pseudo-first-order (PFO) model

Lagergren [74] suggested a PFO equation,

$$q = q_e(1 - e^{-k_1 t}) \quad (14)$$

where  $q$  is the sorbate concentration (mg/g),  $q_e$  is the equilibrium sorbate concentration (mg/g), and  $k_1$  is the rate constant ( $\text{min}^{-1}$ ). The parameters were calculated (Fig. 14) and reported in Table 7.

#### 4.2 Pseudo-second-order (PSO) model

The PSO model is given by McKay et al. [75].

$$q = \frac{q_e^2 k_2 t}{1 + q_e k_2 t} \quad (15)$$

where  $q_e$  (mg/g) is the amount of Cr (VI) adsorbed at equilibrium,  $q$  (mg/g) is the amount of Cr (VI) adsorbed at time  $t$ ,  $k_2$  (g/mg min) is the rate constant of pseudo-II order. The rate constants and  $R^2$  values were evaluated (Fig. 15) and are given in Table 7. Based on the correlation coefficients,  $R^2$ , the PFO model fits better with the experimental data than the PSO model.

#### 4.3 Intra-particle diffusion

Weber [76] proposed the IPD model,

$$q_e = k_d t^{0.5} \quad (16)$$

where  $k_d$  ( $\text{mg/g min}^{-0.5}$ ) is the rate constant. The rate constants of intra-particle diffusion were calculated from Fig. 16. From Table 7, it has been found that the PSO model has a higher  $R^2$  value and low RMSE and MAPE. This indicates that the sorption of Cr (VI) on the sorbent follows first-order kinetic model. Higher values of  $R^2$  show a better fitness of the sorption data [77].

### 5 Reusability of sorbent

Reusability of the biomass offers effective economic benefits and ensures the feasible application of the algal biomass for remediation of metal-contaminated water. The desorption of Cr (VI) was investigated using different strengths of HCl and found that the effective desorption was achieved with 0.4 M HCl [49]. The biosorbent was reused for 5 cycles and the sorbed Cr (VI) was eluted with 0.4 M HCl and was depicted in Fig. 16. Also, in the first 3 cycles, more than 91% of sorbed Cr ions are desorbed from the sorbent. In the 4th and 5th cycles, the cadmium biosorption decreased to less than

80%. This loss of biosorption efficiency with an increase in cycles could be due to the amount of biomass lost. In addition, the possibilities of acid deactivation of surface active sites can inhibit the removal performance [49]. The results indicate that the *Turbinaria ornata* can be reused for five cycles in the sorption of Cr (VI).

### 6 Conclusions

A novel, cost-effective biomass, *Turbinaria ornata*, was used as an adsorbent for the Cr (VI) adsorption. RSM was used to determine the optimal condition of sorption for Cr (VI) onto *Turbinaria ornata*. The optimum conditions were determined as temperature (33.6 °C), sorbent size (0.786 mm), contact time (215 min), agitation speed (117 pm), and adsorbent dose (0.27 g/100 ml) solution. The maximum capacity in sorption was 44.95 mg/g. The adsorption experimental data were analyzed using various isotherm and the results show that the Cr (VI) follows Langmuir. FTIR analyses confirm the involvement of –OH, –COO, and –NH functional group in Cr (VI) adsorption onto *Turbinaria ornata*. Thus, it can be concluded that *Turbinaria ornata* can be effectively employed for the removal Cr (VI), and also, it can be tried for other metals from the effluent stream.

### References

1. Suresh G, Balasubramanian B, Ravichandran N, Ramesh B, Heskamyab, Velmurugan P, Vijayansiva G, Veera ravi A (2021) Bioremediation of hexavalent chromium-contaminated wastewater by *Bacillus thuringiensis* and *Staphylococcus capitis* isolated from tannery sediment. *Biomass Conv Bioref* 11:383–391
2. Jezequel K, Lebeau T (2008) Soil bioaugmentation by free and immobilized bacteria to reduce potentially phytoavailable cadmium. *Bioresour Technol* 99:690–698
3. Wang Q, Song J, Sui M (2011) Characteristic of adsorption, desorption and oxidation of Cr (III) on birnessite. *Energy Pro* 5:1104–1108
4. Sarin V, Pant K (2006) Removal of chromium from industrial waste by using Eucalyptus bark. *Bioresour Technol* 97(1):15–20
5. Adurty S, Sabbu JR (2015) Novel catalytic fluorescence method for speciative determination of chromium in environmental samples. *J Anal Sci Tech* 6(1):1–8
6. Ofudje EA, Awotula AO, Oladipo GO, Williams OD (2014) Detoxification of chromium (VI) ions in aqueous solution via adsorption by raw and activated carbon prepared from sugarcane waste. *Cov J Phy Life Sci* 2(2):110–122
7. Gupta VK, Chandra R, Tyagi I, Verma M (2016) Removal of hexavalent chromium ions using CuO nanoparticles for water purification applications. *J Coll Inter Sci* 478:54–62
8. Rengaraj S, Joo CK, Kim Y, Yi J (2003) Kinetics of removal of chromium from water and electronic process waste water by ion exchange resins: 1200H, 1500H and IRN97H. *J Hazar Mater* 102:257–275

9. Garg VK, Gupta R, Kumar R, Gupta RK (2004) Adsorption of chromium from aqueous solution on treated sawdust. *Bioresour Technol* 92:79–81
10. Moosavirad SM, Sarikhani R, Shahsavani E, Mohammadi SZ (2015) Removal of some heavy metals from inorganic industrial wastewaters by ion exchange method. *J Wat Chem Tech* 37(4):191–199
11. Sarojini G, Venkateshbabu S, Rajamohan N, Senthil Kumar P, Rajasimman M (2021) Surface modified polymer – magnetic – algae nanocomposite for the removal of Chromium – Equilibrium and mechanism studies. *Environ Res* 201:111626
12. Rajasimman M, Sangeetha R, Karthic P (2009) Statistical optimization of process parameters for the extraction of chromium (VI) from pharmaceutical wastewater by emulsion liquid membrane. *Chem Eng J* 150:275–279
13. Rajasimman M, Sangeetha R (2009) Optimization of process parameters for the extraction of Chromium (VI) by emulsion liquid membrane using response surface methodology. *J Hazard Mater* 168:291–297
14. Burakov AE, Galunin EV, Burakova IV, Kucherova AE, Agarwal S, Tkachev AG, Gupta VK (2018) Adsorption of heavy metals on conventional and nanostructured materials for wastewater treatment purposes: a review. *Ecotoxicol Environ Saf* 148:702–712
15. Carmona MER, Da Silva MAP, Leite SGF (2005) Biosorption of chromium using factorial experimental design. *Process Biochem* 40:779–788
16. Deng L, Su Y, Su H, Wang X, Zhu X (2007) Sorption and desorption of lead (II) from wastewater by green algae *Cladophora fascicularis*. *J Hazard Mater* 143:220–225
17. Rajamohan N, Rajasimman M, Rajeshkannan R, Saravanan V (2014) Equilibrium, kinetic and thermodynamic studies on the removal of Aluminum by modified *Eucalyptus camaldulensis* barks. *Alex Eng J* 53(2):409–415
18. Fu F, Wang Q (2011) Removal of heavy metal ions from wastewaters: a review. *J Environ Manage* 92:407–418
19. Rajamohan N, Rajasimman M, Dilipkumar M (2014) Parametric and kinetic studies on biosorption of mercury using modified *Phoenix dactylifera* biomass. *J Taiwan Inst Chem Eng* 45(5):2622–2627
20. Rajamohan N, Rajasimman M (2015) Biosorptive removal of heavy metal onto raw activated sludge: parametric, equilibrium, and kinetic studies. *J Environ Eng* 142(9):C4015002
21. Rajamohan N, Rajasimman M (2015) Biosorption of selenium using activated plant based sorbent – effect of variables, isotherm and kinetic modeling. *Biocatal Agric Biotechnol* 4(4):795–800
22. Gao H, Liu Y, Zeng G, Xu W, Li T, Xia W (2008) Characterization of Cr (VI) removal from aqueous solutions by a surplus agricultural waste rice straw. *J Hazard Mater* 150(2):446–52
23. Rangabhashiyam S, Selvaraju N (2015) Adsorptive remediation of hexavalent chromium from synthetic wastewater by a natural and ZnCl<sub>2</sub> activated *Sterculia guttata* shell. *J Mol Liq* 207:39–49
24. Prasad AG, Abdullah MA (2010) Biosorption of Cr (VI) from synthetic wastewater using the fruit shell of gulmohar (*Delonix regia*): application to electroplating wastewater. *NC State Univ Bioresour* 5(2):838–853
25. Bamukyaye S, Wanasolo W (2017) Performance of egg-shell and fish-scale as adsorbent materials for chromium (VI) removal from effluents of tannery industries in Eastern Uganda. *Open Acc Lib J* 4:1–12. <https://doi.org/10.4236/oalib.1103732>
26. Malwade K, Lataye D, Mhaisalkar V, Kurwadkar S, Ramirez D (2016) Adsorption of hexavalent chromium onto activated carbon derived from *Leucaena leucocephala* waste sawdust: kinetics, equilibrium and thermodynamics. *Inter J Envir Sci Techn* 13(9):2107–2116
27. Sathish T, Vinithkumar NV, Dharani G, Kirubakaran R (2015) Efficacy of mangrove leaf powder for bioremediation of chromium (VI) from aqueous solutions: kinetic and thermodynamic evaluation. *App Wat Sci* 5(2):153–160
28. Parlayici S, Pehlivan E (2015) Natural biosorbents (garlic stem and horse chestnut shell) for removal of chromium (VI) from aqueous solutions. *Environ Monit Asses* 187(2):1–10
29. Pathania D, Sharma A, Srivastava AK (2020) Modelling studies for remediation of Cr (VI) from wastewater by activated *Mangifera indica* bark. *Curr Opin Green Sustain Chem* 3:100034
30. Yang J, Yu M, Chen W (2015) Adsorption of hexavalent chromium from aqueous solution by activated carbon prepared from Longan seed: kinetics, equilibrium and thermodynamics. *J Ind Eng Chem* 21:414–422
31. Rajasimman M, Murugaiyan K (2010) Optimization of process variables for the biosorption of chromium using *Hypnea Valentiae*. *Nova Biotechnologica* 10(2):107–115
32. Jayakumar R, Rajasimman M, Karthikeyan C (2014) Sorption of hexavalent chromium from aqueous solution using marine green algae *Halimeda gracilis*: Optimization, equilibrium, kinetic, thermodynamic and desorption studies. *J Environ Chem Eng* 2:1261–1274
33. Jayakumar R, Rajasimman M, Karthikeyan C (2014) Optimization studies on the Sorption of Cu (II) from aqueous solution using marine brown algae: *Sargassum myriocystum*. *Int J ChemTech Res* 6(10):4525–4532
34. Jayakumar R, Rajasimman M, Karthikeyan C (2015) Optimization, equilibrium, kinetic, thermodynamic and desorption studies on the sorption of Cu (II) from an aqueous solution using marine green algae: *Halimeda gracilis*. *Ecotox Environ Safe* 121:199–210
35. Aravind J, Kanmani P, Devisri AJ, Dhivyalakshmi S, Raghavprasad M (2015) Equilibrium and kinetic study on chromium (VI) removal from simulated waste water using gooseberry seeds as a novel biosorbent. *Glob J Envir Sci Manag* 1(3):233–244
36. Jayakumar R, Rajasimman M, Karthikeyan C (2015) Sorption and desorption of hexavalent chromium using a novel brown marine algae *Sargassum myriocystum*. *Korean J Chem Eng* 32(10):2031–2046
37. Jayakumar R, Rajasimman M, Karthikeyan C (2021) Column studies on sorption of Cr (VI) from aqueous and electroplating wastewater using acid-treated marine brown algae *Sargassum myriocystum*. *Energ Source Part A*. <https://doi.org/10.1080/15567036.2019.1680768>
38. APHA (1995) Standard methods for the examination of water and wastewater, 16th edn. American Public Health Association, Washington
39. Montgomery DC (2001) Design and analysis of experiments, 5th edn. John Wiley and Sons Inc., New York
40. Sarojini G, Venkateshbabu S, Rajasimman M (2021) Facile synthesis and characterization of polypyrrole - iron oxide – seaweed (PPy-Fe<sub>3</sub>O<sub>4</sub>-SW) nanocomposite and its exploration for adsorptive removal of Pb(II) from heavy metal bearing water. *Chemosphere* 278:130400
41. Jayakumar V, Govindaradjane S, Rajamohan N, Rajasimman M (2021) Sustainable removal of cadmium from contaminated water using green algae – optimization, characterization and modeling studies. *Environ Res* 199:111364
42. Muthu Kumara Pandian A, Gopalakrishnan B, Rajasimman M, Rajamohan N, Karthikeyan C (2021) Green synthesis of bio-functionalized nano-particles for the application of copper removal – characterization and modeling studies. *Environ Res* 197:111140
43. Jayakumar V, Govindaradjane S, Rajasimman M (2021) Efficient adsorptive removal of Zinc by green marine macro alga *Caulerpa scalpelliformis* – characterization, optimization, modeling, isotherm, kinetic, thermodynamic, desorption and regeneration studies. *Surfaces Interfaces* 22:100798
44. Langmuir I (1916) The adsorption of gases on plane surface of glass, mica and platinum. *J Am Chem Soc* 40:1361–1368

45. Freundlich HMF (1906) Over the adsorption in solution. *J Phys Chem* 57:385–470
46. Dubinin MM (1960) The potential theory of adsorption of gases and vapors for adsorbents with energetically non-uniform surface. *Chem Rev* 60:235–266
47. Temkin MJ, Pyzhev V (1940) Kinetics of ammonia synthesis on promoted Iron catalysts. *ctaphysiochem URSS* 12:217–256
48. Rajeshkannan R, Rajamohan N, Rajasimman M (2010) Optimization, equilibrium and kinetic studies on removal of acid blue 9 using brown marine algae *turbinaria conoids*. *Biodegradation* 21:713–727
49. Jayakumar V, Govindaradjane S, Rajasimman M (2019) Isotherm and kinetic modeling of sorption of cadmium onto a novel red algal sorbent, *Hypnea musciformis*. *Model Earth Syst Environ* 5:793–805
50. Rajasimman M, Murugaiyan K (2012) Application of the statistical design for the sorption of lead by *Hypnea Valentiae*. *J Adv Chem Eng* 2:1–7. <https://doi.org/10.4303/jace/A110402>
51. Bhatti IA, Ahmad N, Iqbal N, Zahid M, Iqbal M (2017) Chromium adsorption using waste tire and conditions optimization by response surface methodology. *J Environ Chem Eng* 5(3):2740–2751
52. Pakade VE, Tavengwa Nikita T, Madikizela Lawrence M (2019) Recent advances in hexavalent chromium removal from aqueous solutions by adsorptive methods. *RSC Adv* 9:26142–26164
53. Pintor M-J, Jean-Marius C, Jeanne-Rose V, Taberna P-L, Simon P, Gamby J, Gadiou R, Sarra G (2013) Preparation of activated carbon from *Turbinaria turbinata* seaweeds and its use as super-capacitor electrode materials. *C R Chim* 16(1):73–79
54. Pathania D, Sharma A, Srivastava AK (2020) Modelling studies for remediation of Cr (VI) from wastewater by activated *Mangifera indica* bark. *Curr Res Green Sustain Chem* 3:100034
55. Murphy V, Tofail SAM, Hughes H, McLoughlin P (2009) A novel study of hexavalent chromium detoxification by selected seaweed species using SEM-EDX and XPS analysis. *Chem Eng J* 148:425–433
56. Pakade VE, Ofomaja NTD, AE, (2017) Biosorption of hexavalent chromium from aqueous solutions by Macadamia nutshell powder. *Appl Water Sci* 7:3015–3030
57. Ntuli TD, Pakade VE (2020) Hexavalent chromium removal by polyacrylic acid-grafted Macadamia nutshell powder through adsorption–reduction mechanism: Adsorption isotherms, kinetics and thermodynamics. *Chem Eng Commun* 207(3):279–294
58. Nabila Al-Rashdi, Rajamohan N, Ramachandran KP (2017) Synthesis and application of *Sargassum ilicifolium* based biomass for the selective removal of phenol. *Biocatal Agric Biotechnol* 9:236–239
59. Akram M, Bhatti HN, Iqbal M, Noreen S, Sadaf S (2017) Bio-composite efficiency for Cr (VI) adsorption: kinetic, equilibrium and thermodynamics studies. *J Environ Chem Eng* 5(1):400–411
60. Lodeiro P, Barriad JL, Herrero R, Sastre de Vicente ME (2006) The marine macroalga *Cystoseira baccata* as biosorbent for cadmium (II) and lead (II) removal: kinetic and equilibrium studies. *Environ Pollut* 142:264–273
61. Sari M, Tuzen M, Soylak (2007) Adsorption of Pb (II) and Cr (III) from aqueous solution on Celtek clay. *J Hazar Mater* 144:41–46
62. Parlayici Ş, Pehlivan E (2019) Comparative study of Cr (VI) removal by bio-waste adsorbents: equilibrium, kinetics, and thermodynamic. *J Anal Sci Technol* 10:15
63. Wanees SA, Ahmed AM, Adam MS, Mohamed MW (2012) Adsorption studies on the removal of hexavalent chromium-contaminated wastewater using activated carbon and bentonite. *Asian J Chem* 2:95–105
64. Marjanovic V, Lazarevic S, Jankovic-Castvan I, Jokic B, Janackovic DJ, Petrovic R (2013) Adsorption of chromium (VI) from aqueous solutions onto amine functionalized natural and acid-activated sepiolites. *Appl Clay Sci* 80–81:202–210
65. Bamukyaye S, Wanasolo W (2017) Performance of egg-shell and fish-scale as adsorbent materials for chromium (VI) removal from effluents of tannery industries in Eastern Uganda. *Open Acc Lib J* 4(8):1
66. Mekonnen E, Yitbarek M, Soreta TR (2015) Kinetic and thermodynamic studies of the adsorption of Cr (VI) onto some selected local adsorbents. *Sou African J Chem* 68:45–52
67. Bayuo J, Pelig-Ba KB, Abukari MA (2019) Adsorptive removal of chromium (VI) from aqueous solution unto groundnut shell. *Appl Water Sci* 9:107
68. Hariharan A, Harini V, Sandhya S, Rangabhashiyam S (2020) Waste Musa acuminata residue as a potential biosorbent for the removal of hexavalent chromium from synthetic wastewater. *Biomass Conv Bioref*. <https://doi.org/10.1007/s13399-020-01173-3>
69. Amaku JF, Ogundare SA, Akpomie KG, Ngwu CM, Conradie J (2021) Sequestered uptake of chromium(VI) by *Irvingia gabonensis* stem bark extract anchored silica gel. *Biomass Conv Bioref*. <https://doi.org/10.1007/s13399-021-01563-1>
70. Gupta GK, Mondal MK (2020) Mechanism of Cr (VI) uptake onto sawgan sawdust derived biochar and statistical optimization via response surface methodology. *Biomass Conv Bioref*. <https://doi.org/10.1007/s13399-020-01082-5>
71. Deepa A, Singh A, Singh A, Mishra BK (2021) An experimental approach for the utilization of tannery sludge-derived *Bacillus* strain for biosorptive removal of Cr (VI) -contaminated wastewater. *Environ Sci Pollut Res* 28:9864–9876
72. Chandipatra TasrinShahnaz (2020) SenthilmuruganSubbiah, SelvarajuNarayanasamy (2020) Comparative assessment of raw and acid-activated preparations of novel *Pongamia pinnata* shells for adsorption of hexavalent chromium from simulated wastewater. *Environ Sci Pollut Res* 27:14836–14851
73. Jang Eun-Hye, Pack SeungPil, Kim Il, Chung Sungwook (2020) A systematic study of hexavalent chromium adsorption and removal from aqueous environments using chemically functionalized amorphous and mesoporous silica nanoparticles. *Sci Rep* 10:5558
74. Lagergren SY (1898) Zur Theorie der sogenannten Adsorption gelöster Stoffe, *Kungliga Svenska Vetenskapsakad. Handlingar* 24:1–3
75. McKay G, Ho YS, Ng JCY (1999) Biosorption of copper from waste waters: a review. *Separ Purif Rev* 28(1):87–125
76. Weber W, Morris J (1963) Kinetics of adsorption on carbon from solutions. *J Sanit Eng Div Am Soc Civ Eng* 89:31–60
77. Titchou FE, Akbour RA, Assabbane A, Hamdani M (2020) Removal of cationic dye from aqueous solution using Moroccan pozzolana as adsorbent: isotherms, kinetic studies, and application on real textile wastewater treatment. *Ground w Sustain* 11:100405

**Publisher's note** Springer Nature remains neutral with regard to jurisdictional claims in published maps and institutional affiliations.